JOC Featured Article

pubs.acs.org/joc

Unsymmetrical Cruciforms

Juan Tolosa, Kyril M. Solntsev, Laren M. Tolbert, and Uwe H. F. Bunz*

School of Chemistry and Biochemistry, Georgia Institute of Technology, 901 Atlantic Drive, Atlanta, Georgia 30332-0400

uwe.bunz@chemistry.gatech.edu

Received September 15, 2009

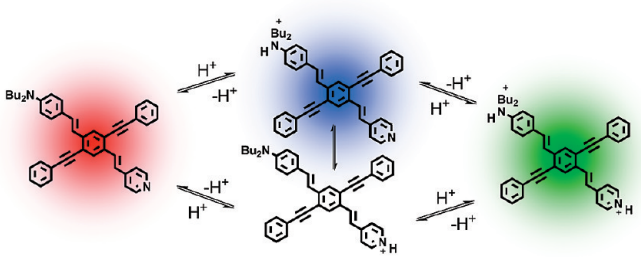

Five new, unsymmetrical 1,4-distyryl-2,5-bisphenylethynylbenzenes (cruciforms, XF) have been prepared by a sequential Horner reaction of the bisphosphonate of 2,5-diiodo-1,4-xylene with two different aromatic aldehydes. The obtained diiodide was coupled to phenylacetylene under Sonogashira conditions with $(Ph_3P)_2PdCl_2$ as catalyst. The resulting XFs carry dibutylamino, pyridyl, cyano, and diphenylamino residues on their styryl arms to give rise to donor−, acceptor−, and donor−acceptor-substituted XFs. The optical properties of these XFs were investigated. Titration studies using trifluoroacetic acid tracked changes in the electronic structure of the XFs upon protonation. Donor XFs display a blue shift in absorption and emission upon protonation, while the pyridyl-substituted XF displays red shift in absorption and emission upon protonation. In the case of the donor−acceptor XF carrying a pyridyl and an aminostyryl arm, the first protonation occurs either on the pyridine or on the dibutylamino arm; a red shift is seen in absorption (for the former) and a blue shift is observed in emission (for the latter). The titration studies indicate that the protonated XFs do not display *kinetic* photoacidity when operating either in dichloromethane or acetonitrile solutions. The trends observed for protonation were mirrored when the XFs bind to metal cations. While the binding constants of the metal cations to the XFs were lower than for that for protons, as in some cases full metalation of the XF could not be obtained, the results were qualitatively the same. We did not find *dynamic* excited-state decomplexation events in the XFs that we have investigated. The XFs, stilbene derivatives, are different from other reported, similarly structured fluorophores as they show significant ratiometric changes in emission upon metal complexation; thus, distyrylbenzene-derived fluorophores may be, in the end, viable choices as platforms for metal ion detection.

Introduction

We disclose in this manuscript the synthesis as well as photophysical, acidochromic, and metallochromic/metallofluorophoric properties of the five cruciform fluorophores (1,4-distyryl-2,5-bisarylethynylbenzenes, XF) **1**−**5** and compare their properties to those of the corresponding symmetrical XFs **6**−**8**.[1]

Cruciform $(XF)^{2-6}$ is a catch-all term for diaxial chromophores in which the properties of the two axes can be

(1) (a) Wilson, J. N.; Smith, M. D.; Enkelmann, V.; Bunz, U. H. F. *Chem. Commun.* **2004**, 1700–1701. (b) Wilson, J. N.; Bunz, U. H. F. *J. Am. Chem. Soc.* **2005**, *127*, 4124–4125. (c) Zucchero, A. J.; Wilson, J. N.; Bunz, U. H. F. *J. Am. Chem. Soc.* **2006**, *128*, 11872–11881. (d) McGrier, P. L.; Solntsev, K. M.; Miao, S.; Tolbert, L. M.; Miranda, O. R.; Rotello, V. M.; Bunz, U. H. F. *Chem.—Eur. J.* **2008**, *14*, 4503–4510.

(2) (a) Miao, Q.; Chi, X. L.; Xiao, S. X.; Zeis, R.; Lefenfeld, M.; Siegrist, T.; Steigerwald, M. L.; Nuckolls, C. *J. Am. Chem. Soc.* **2006**, *128*, 1340–1345. (b) Klare, J. E.; Tulevski, G. S.; Sugo, K.; de Picciotto, A.; White, K. A.; Nuckolls, C. *J. Am. Chem. Soc.* **2003**, *125*, 6030–6031.

(3) (a) Marsden, J. A.; Miller, J. J.; Shirtcliff, L. D.; Haley, M. M. *J. Am. Chem. Soc.* **2005**, *127*, 2464–2476. (b) Spitler, E. L.; Shirtcliff, L. D.; Haley, M. M. *J. Org. Chem.* **2007**, *72*, 86–96. (c) Spitler, E. L.; Haley, M. M. *Tetrahedron* **2008**, *64*, 11469–11474. (d) Spitler, E. L.; Monson, J. M.; Haley, M. M. *J. Org. Chem.* **2008**, *73*, 2211–2223.

DOI: 10.1021/jo901961a Published on Web 10/27/2009

SCHEME 1. Synthesis of 1−5

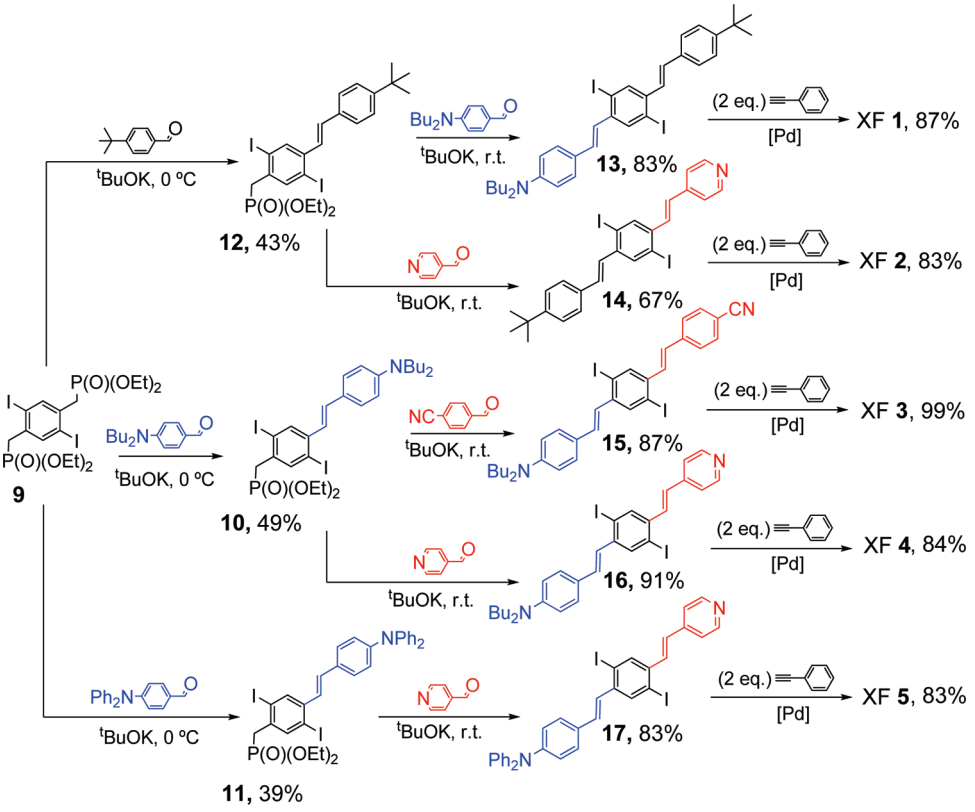

manipulated independently. In most XFs, the diaxial character leads, upon suitable decoration with auxochromic substituents, to spatially separated and therefore independently addressable frontier molecular orbitals.[7] Unusual spatially resolved electronic properties result. We previously investigated XFs **6**−**8** and demonstrated that these are attractive metalloresponsive and acidochromic dyes with a rare two-stage sensory response.[1,8]

However, there was a cluster of questions that could not be addressed with the symmetrical XFs **6**−**8**. Are the partially protonated species stemming from **6**−**8** spectroscopically too similar to the spectra of the fully protonated derivatives or fully nonprotonated or are the subsequent protonation steps faster than the first one? Is there an influence of different conjugative pathways upon changing the topology of the donor and acceptor substituents and their frontier molecular orbitals? Is there evidence for excited-state decomplexation or enhanced complexation upon binding of metal cations to **1**−**5**?[9−11] Conversely, will excited-state photoacidity be enhanced?[9] In searching for answers to these questions, we note that the XFs **1**−**5** are better suited to do this, as multiple complexation of identical binding units occuring in **6**−**8** can be excluded.[10,11]

Results and Discussion

Synthesis. Scheme 1 displays the synthesis of **1**−**5**. The challenging issue was the preparation of the unsymmetrical stilbenes **10**−**12**. The most straightforward way to obtain these targets was to react **9** with 1 equiv of KO^{t}Bu at 0 °C, add the first aldehyde, warm to room temperature, add another 1 equiv of KO^{t}Bu, and add the second aldehyde. These reactions were readily performed in one pot. The Horner reaction of the more electron-rich aldehyde was performed first. The intermediates were obtained in yields between 25 and 41%, less than the statistically expected yield of 50%. We attribute the decreased yield to the increased reactivity of the intermediate styrene derivative, giving rise to the formation of a significant amount of the two symmetrical Horner products. The overall yields of this mixed Horner reaction was >90%, and the products were conveniently separated by column chromatography.[12] The introduction of the secondary axis was achieved by coupling of **10**−**12** to

(4) (a) Kang, H.; Evmenenko, G.; Dutta, P.; Clays, K.; Song, K.; Marks, T. J. *J. Am. Chem. Soc.* **2006**, *128*, 6194–6205. (b) Hu, K.; Zhu, P. W.; Yu, Y.; Facchetti, A.; Marks, T. J. *J. Am. Chem. Soc.* **2004**, *126*, 15974–15975.

(5) Grunder, S.; Huber, R.; Horhoiu, V.; Gonzalez, M. T.; Schonenberger, C.; Calame, M.; Mayor, M. *J. Org. Chem.* **2007**, *72*, 8337–8344.

(6) (a) Zen, A.; Bilge, A.; Galbrecht, F.; Alle, R.; Meerholz, K.; Grenzer, J.; Neher, D.; Scherf, U.; Farrell, T. *J. Am. Chem. Soc.* **2006**, *128*, 3914–3915. (b) Bilge, A.; Zen, A.; Forster, M.; Li, H. B.; Galbrecht, F.; Nehls, B. S.; Farrell, T.; Neher, D.; Scherf, U. *J. Mater. Chem.* **2006**, *16*, 3177–3182.

(7) Wilson, J. N.; Josowicz, M.; Wang, Y. Q.; Bunz, U. H. F. *Chem. Commun.* **2003**, 2962–2963.

(8) (a) Detert, H.; Schmitt, V. *J. Phys. Org. Chem.* **2006**, *19*, 603–607. (b) Detert, H.; Stalmach, U.; Sugiono, E. *Synth. Met.* **2004**, *147*, 227–231.

(9) Tolbert, L. M.; Solntsev, K. M. *Acc. Chem. Res.* **2002**, *35*, 19–27.

(10) (a) Pond, S. J. K.; Tsutsumi, O.; Rumi, M.; Kwon, O.; Zojer, E.; Bredas, J. L.; Marder, S. R.; Perry, J. W. *J. Am. Chem. Soc.* **2004**, *126*, 9291–9306. (b) Valeur, B.; Leray, I. *Coord. Chem. Rev.* **2000**, *205*, 3–40.

(11) (a) Bourson, J.; Valeur, B. *J. Phys. Chem.* **1989**, *93*, 3871–3876. (b) Martin, M. M.; Plaza, P.; Meyer, Y. H.; Badaoui, F.; Bourson, J.; Lefevre, J. P.; Valeur, B. *J. Phys. Chem.* **1996**, *100*, 6879–6888. (c) Ley, C.; Lacombat, F.; Plaza, P.; Martin, M. M.; Leray, I.; Valeur, B. *Chem. Phys. Chem.* **2009**, *10*, 276–281. (d) Grynkiewicz, G.; Poenie, M.; Tsien, R. Y. *J. Biol. Chem.* **1985**, *260*, 3440–3450.

(12) Horner, L.; Hoffmann, H.; Wippel, H. G.; Klahre, G. *Chem. Ber.* **1959**, *92*, 2499–2505.

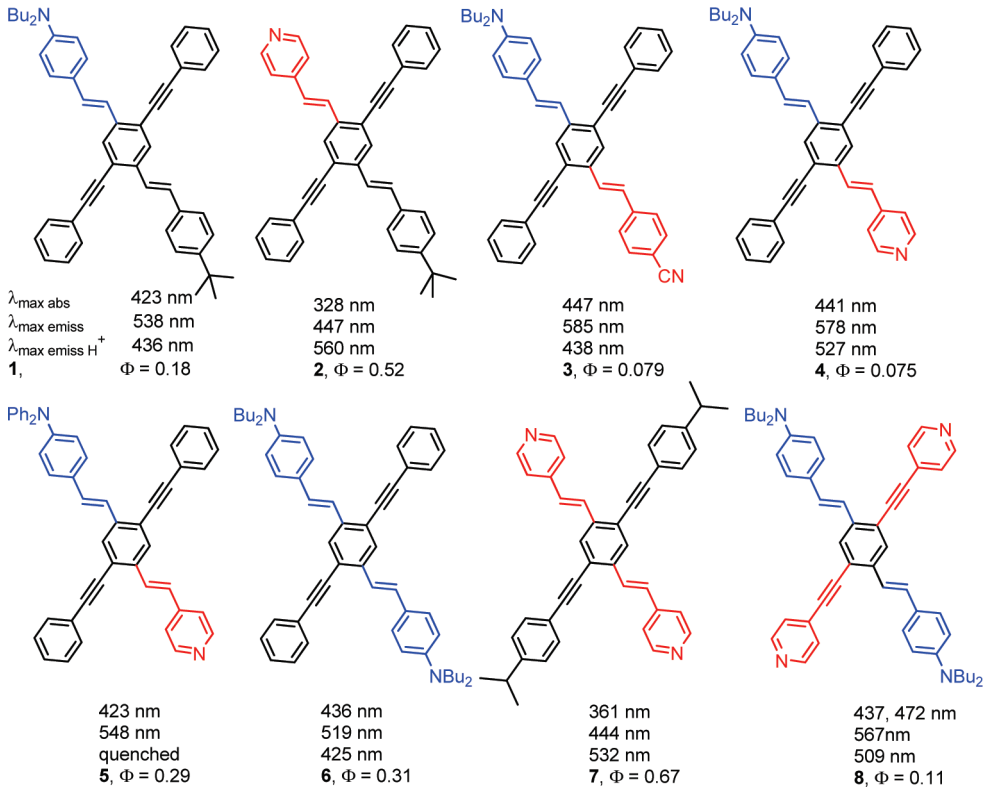

FIGURE 1. Molecular structure of **1**−**8** and their photophysical properties recorded in dichloromethane.

phenylacetylene to give the XFs **1**−**5** in yields between 80 and 92% as yellow to orange crystalline materials.

Photophysics. Figure 1 displays the general photophysical properties of **1**−**5**, while Figure 2 displays the solvent-dependent emission of the XFs **1**−**5**. The absorption maxima of **1**−**5** are almost independent upon the solvent used, while the emission maxima change significantly depending upon the solvent. The absorption and emission spectra of **1**−**5** were taken in a variety of solvents (see the Supporting Information) to construct simplified Lippert−Mataga plots (Figure 3),[13] where Δf, the Lippert−Mataga solvent parameter, is defined as

$$\Delta f = [(\varepsilon - 1)/(2\varepsilon + 1) - (n^2 - 1)/(2n^2 + 1)] \qquad (1)$$

The slope of the best fit indicates the charge-transfer character of the excited states in the molecules **1**−**5**. We find, not unexpectedly, that compound **4** has the largest charge-transfer character in the excited state, due to significant donor−acceptor character. Interestingly, the donor-substituted **1** has a higher charge-transfer character than the acceptor-substituted compound **2**, while the donor−acceptor-substituted model compounds **3** and **5** display an intermediate degree of charge transfer in the excited state as roughly expected from the substituent patterns. For the compounds carrying a dibutylamino group (**1**, **3**−**5**) a small but detectable blue-shifted band was observed upon excitation at 310 nm. The appearance of this band cannot be explained by the typical LE-TICT scenario, since the "LE" peak is bluer than the major emission peak in *n*-hexane. For another reason, the fluorescence quantum yield in acetonitrile is too high to be attributed to TICT emission. An alternative explanation could be the emission from the monoprotonated species, as shown below. However, the peak did not disappear upon addition of a large access of triethylamine. Currently, we are investigating the nature of this weak emission but will omit it in the current publication since it is not critical for the understanding of acidochromic and metalloresponsive properties of novel cruciforms.

Figure 4 displays the absorption and emission spectra of **1**−**5** in acetonitrile upon exposure of an increasing amount of trifluoroacetic acid. The full titration traces are displayed in the Supporting Information. For simplicity, only representative traces are shown in Figure 4.

Since all of the prepared XFs have basic nitrogen groups, protonation should change absorption and/or emission significantly. Addition of trifluoroacetic acid to **1** leads to a blue shift in emission as well as in absorption, surprisingly similar to that observed to the symmetrical compound **6** (Figure 1). Compound **2** by the same token should be analogous to **7**, and again, the spectral responses toward protonation in absorption and emission are comparable. A significant red shift is observed, and the emission intensity of the protonated species is very low. The compounds **3** and **5** represent model compounds, and the addition of TFA to **3** leads to strongly blue emissive species, in which the dibutylamino group is protonated, while addition of TFA to **5**, which is already a donor−acceptor system, leads to a significantly increased donor−acceptor character, as the electron-accepting pyridine unit is protonated. A red shift in absorption results, while the emission is quenched. As a general note, XF species

(13) (a) Lippert, E. *Z. Naturforsch., Part A* **1955**, *10*, 541–545. (b) Lippert, E.; Moll, F. *Z. Elektrochem.* **1954**, *58*, 718–724. (c) Mataga, N.; Kaifu, Y.; Koizumi, M. *Bull. Chem. Soc. Jpn.* **1956**, *29*, 465–470. (d) Reichardt, C. *Chem. Rev.* **1994**, *94*, 2319–2358.

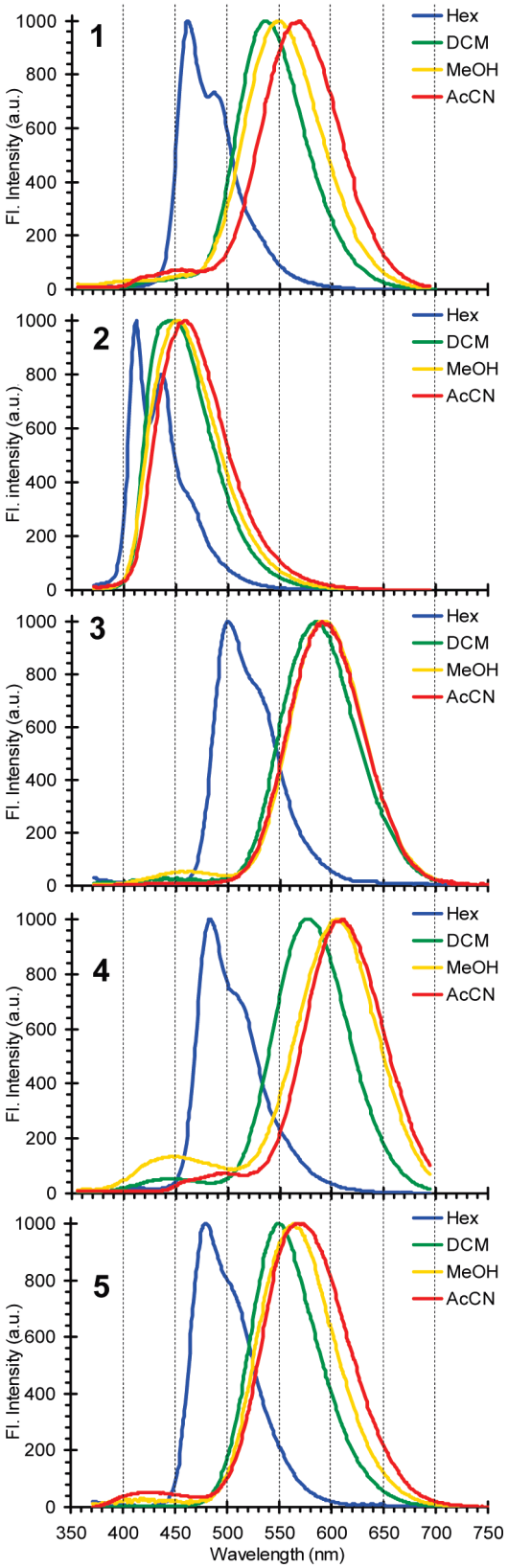

FIGURE 2. Vis emission spectra of **1**−**5** in four different solvents.

with red-shifted emission tend to display lower emissive quantum yields. Reasons for the decreased quantum yield are perhaps vibronic coupling of ground and excited states

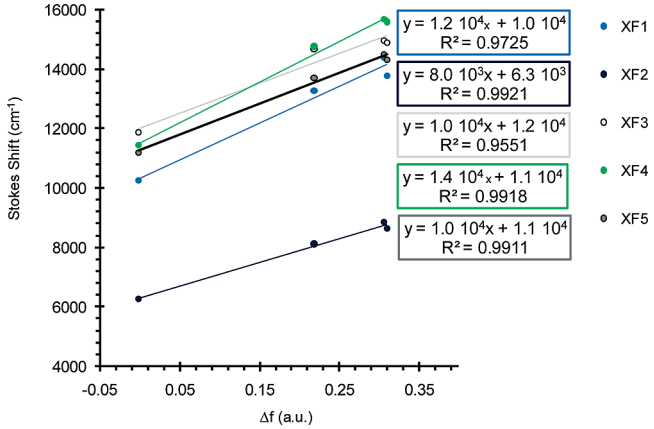

FIGURE 3. Mataga−Lippert plot of XFs **1**−**5**.

(energy gap law) or overtone coupling of the XFs to the solvents. Other reasons could be the twisting of the aromatic system that would lead to nonemissive TICT states.[14]

The most interesting case is "push−pull" XF **4**. The absorption and emission spectra of **4** resemble those of **8**. The emission quantum yield of **4** (Φ = 0.075) is slightly lower than that of **8** (Φ = 0.11). The titration of this compound with TFA gives surprising results. Upon addition of TFA a red-shift in absorption occurs and then upon addition of more TFA a blue shift. The final absorption is centered around 381 nm. In emission the situation is reversed. Upon addition of TFA first a weak blue-shifted band appears, then upon addition of more TFA a strongly fluorescent band at 541 nm arises. One should note that at log[TFA] = −4.3 a formally large negative Stokes shift results. The absorption is centered at 495 nm, while the emission is centered at 437 nm. What is the explanation for this seemingly contradictory behavior? Deconvolution of the titration traces by the singular value decomposition (SVD)[15] reveals three species. The simulated absorption and emission spectra as well as their molar fraction present (Figure 5, observed in absorption, top, and emission, bottom) of which are shown in Figures 5 and 6. The blue spectra are from the unprotonated XF and are unsurprising. The red traces represent the spectra of the doubly protonated XF. Both of these are in accord with what would be expected from such an XF. However, the green traces can only be explained if one assumes the pyridine nitrogen is predominantly protonated in the first step. That would lead to a situation reminiscent of the one found for **5**, where a red shift in absorption and a total quenching in emission results. The emission tells a different story. It is similar to that for **3**; i.e., a blue shift in emission is observed, even though its intensity is much lower. Figure 7 reconciles the processes. Upon addition of TFA either the pyridine (majority) or the dibutylamino group (minority) of **4** is protonated. The two protonated species are in equilibrium with each other. From the UV−vis spectrum and the emission spectrum one would conclude that the main form is $\mathbf{4H^+b}$ as the fluorescence intensity is low but the intensity of the charge-transfer band in absorption that we assign to $\mathbf{4H^+b}$ is quite intense, explaining the observed spectroscopic features consistently and without convoluted

(14) Rettig, W. *Angew. Chem., Int. Ed. Engl.* **1986**, *25*, 971–988.
(15) Program DATAN, www.multid.se.

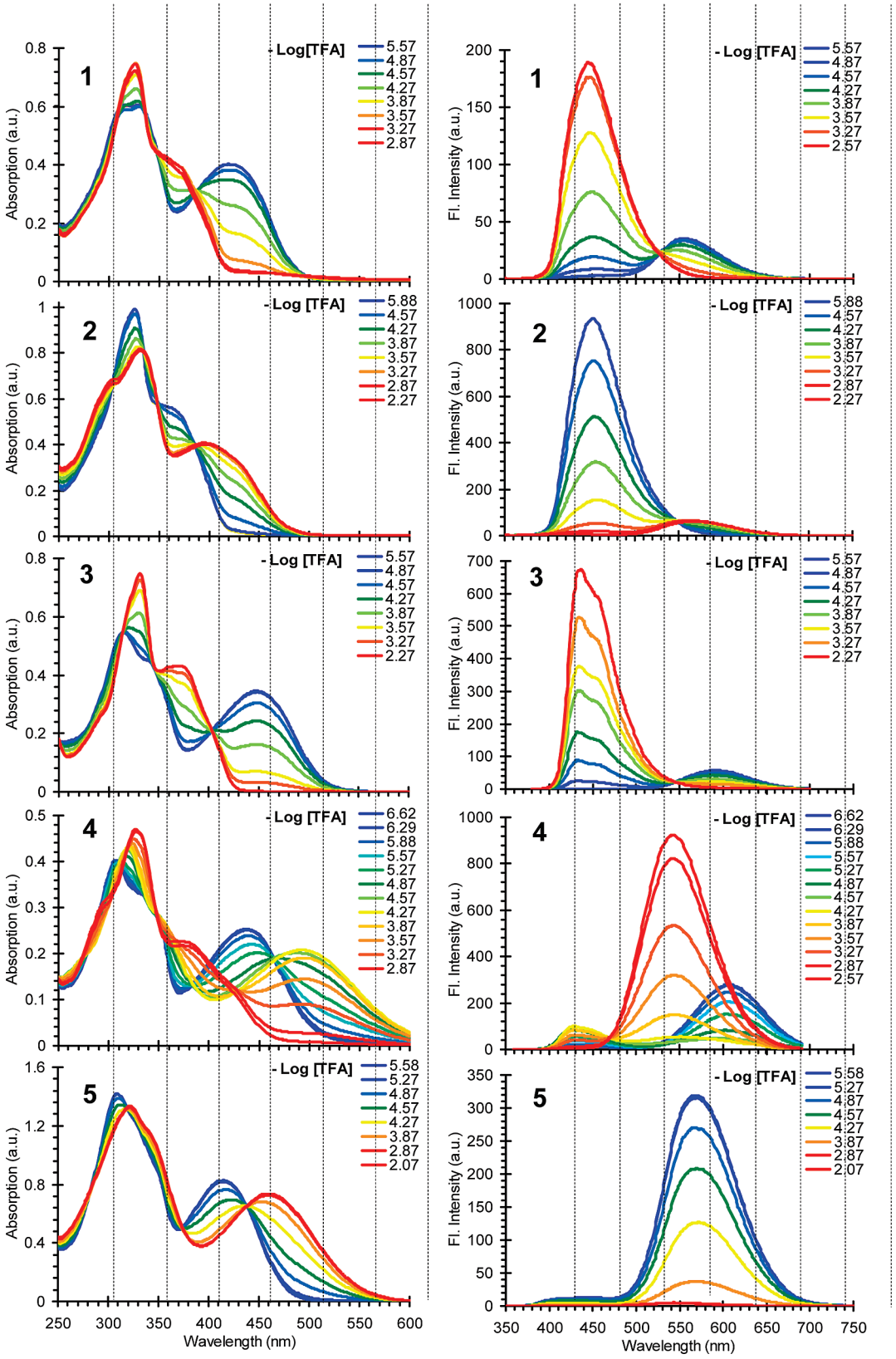

FIGURE 4. UV/vis absorption and emission spectra of **1**−**5** in acetonitrile upon titration with trifluoroacetic acid. Excitation wavelength was 325 nm.

explanations. As the ratio between $4H^+$**a** and $4H^+$**b** represents an equilibrium, their species distribution is reflected both in absorption as well as in emission, even though different species are observed.

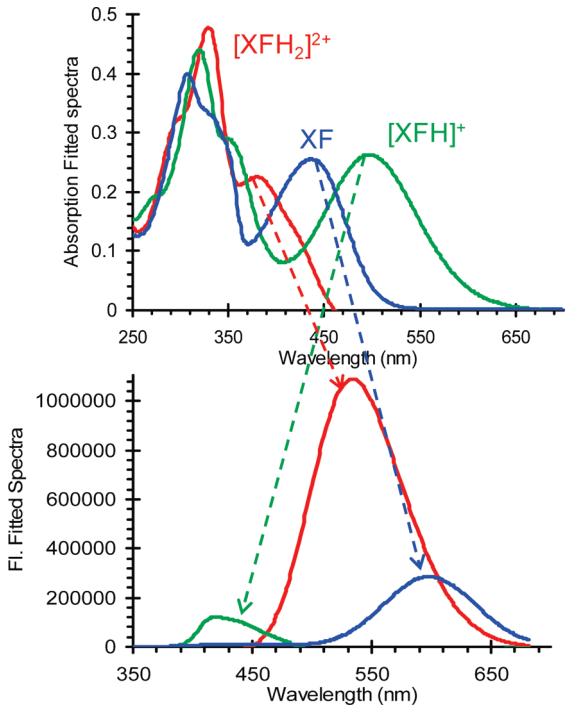

FIGURE 5. Analysis of the titration of **4**. Top: Fitted UV/vis absorption spectra. Bottom, fitted emission spectra upon exposure of **4** to trifluoroacetic acid; $\lambda_{maxexcitation} = 310$ nm.

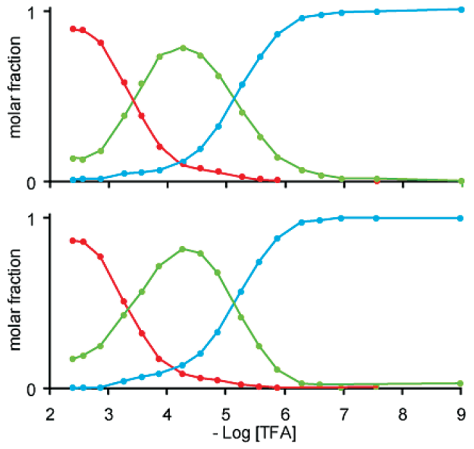

FIGURE 6. Species distribution of **4** upon protonation, observed by absorption (top) and emission (bottom) spectroscopy. Red: deprotonated species. Blue: unprotonated species. Green: monoprotonated species.

The spectroscopic properties of **4** differ significantly from those of the XF **8** in the sense that, as in **8**, the protonation of the dibutylaniline group occurs first, and the protonation of the pyridine unit subsequently. Pyridines and dibutylanilines in **8** have sufficiently large differences in pK_a values, so that both in absorption and in emission the di- and the tetraprotonated species can be discerned, and that only one type of diprotonated species, resulting from protonation of the dibutylanilines, occurs. In **4** the situation is more complex, as the pK_a values of the pyridine and the dibutylaniline appear to be quite similar or the pK_a of the pyridinium is even larger due to the mesomeric effect of the electron donating aniline unit. Therefore protonation of the pyridine and the dibutylaniline are competitive.

For a more detailed study of the photophysical properties of **4** in solutions of variable acidity, and to reveal possible hidden or weakly emitting states we investigated its excitation−emission matrix (EEM). EEM spectroscopy has recently emerged as an effective method for spectroscopic characterization of multifluorophoric systems.[16−19] We collected the emission spectra of the fluorophore at room temperature scanning the excitation wavelength from 250 to 580 nm at 5 nm increments. In Figure 8, the emission spectra of the **4** in acetonitrile in the presence of various amounts of TFA are presented, which allowed the observation of every emission band and its correlation to the appropriate excitation wavelength. As predicted by previous observations, only three emitting species exist and interconvert in solutions of **4** depending on their TFA concentrations.

The apparent ΔpK_a values (strictly speaking these are $-\log \beta$ values, i.e., binding constants, as the titrations were performed in acetonitrile) as measured in absorption and emission and obtained by SVD, are similar for **4**. To see if this was representative for the XFs, we also analyzed the absorption as well as the emission traces of **1**−**3** and **5** upon addition of TFA by SVD. Table 1 displays the $-\log \beta$ values as obtained by UV−vis and emission spectroscopies. In all cases, the coincidence of the values is very good. This is of interest, as it suggests that, at least kinetically, the distyrylbenzene derivatives do not show enhanced photoacidity as do some other aromatic amines in nonaqueous solvents.[20] As we have observed in other contexts,[9] proton transfer is extraordinarily dependent upon solvent reorganization as well as orientation of the proton carrier (base), resulting in a significant entropic barrier to such deprotonation.

The nature of the involved processes is of interest as they might shed light on the "excited state decomplexation hypothesis" that is proposed for aminostyrylbenzene derivatives and their fluorescence response toward metal cations. This hypothesis states that in the excited state aminostilbenes and their relatives form quinoidal resonance structures in which the electron pair in the aniline unit(s) is transferred to the stilbene skeleton and not available for metal coordination.[21] A consequence of this behavior is the observation that addition of metal salts to such species lead to significant changes (mostly blue shift) in absorption but to only very small changes in emission. Perry et al. have demonstrated this effect in an elegant paper, in which they investigated crown-ether appended dicyanodistyrylbenzenes and their optical changes upon metal-ion binding. Inspired by their

(16) Weber, G. *Nature* **1961**, *190*, 27–29.
(17) Clower, C.; Solntsev, K. M.; Kowalik, J.; Tolbert, L. M.; Huppert, D. *J. Phys. Chem. A* **2002**, *106*, 3114–3122.
(18) Gill, D. M.; Wright, J. C.; McCaughan, L. *Appl. Phys. Lett.* **1994**, *64*, 2483–2485.
(19) Dong, J.; Solntsev, K. M.; Tolbert, L. M. *J. Am. Chem. Soc.* **2009**, *131*, 662–670.
(20) (a) Urban, W.; Weller, A. *Ber. Bunsen Ges.* **1963**, *67*, 787–791. (b) Demyashkevich, A. B.; Ivanova, L. L.; Kiselevich, V. R.; Kuzmin, M. G. *Sov. J. Chem. Phys.* **1990**, *5*, 759–767. (c) Ivanova, L. L.; Demyashkevich, A. B.; Kuzmin, M. G. *High Energy Chem.* **1984**, *18*, 99–101. (d) Ivanova, L. L.; Demyashkevich, A. B.; Kuzmin, M. G. *High Energy Chem.* **1985**, *19*, 48–52.
(21) (a) Letard, J. F.; Lapoyade, R.; Rettig, W. *Pure Appl. Chem.* **1993**, *65*, 1705–1712. (b) Mathevet, R.; Jonusauskas, G.; Rulliere, C.; Letard, J. F.; Lapouyade, R. *J. Phys. Chem.* **1995**, *99*, 15709–15713.

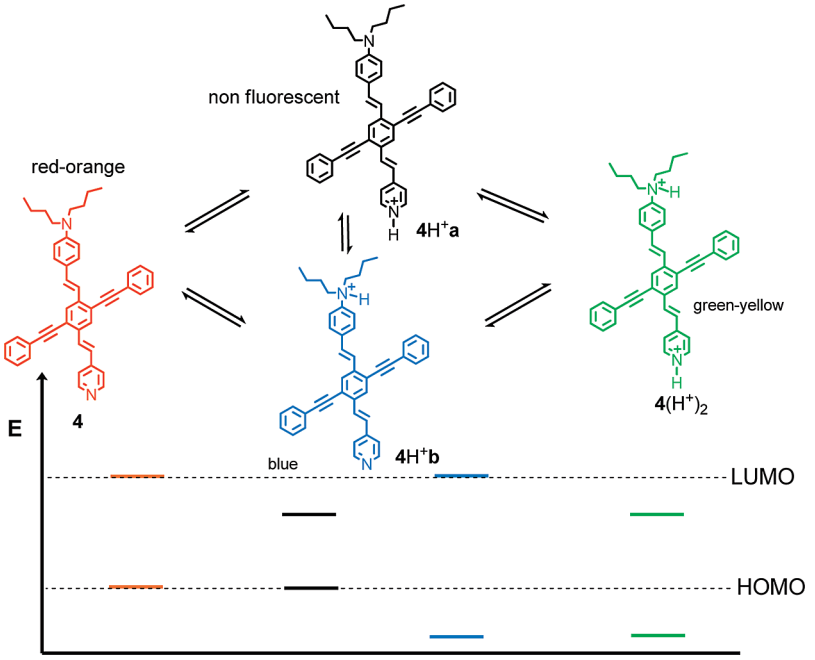

FIGURE 7. Analysis of the interaction of protons with **4**.

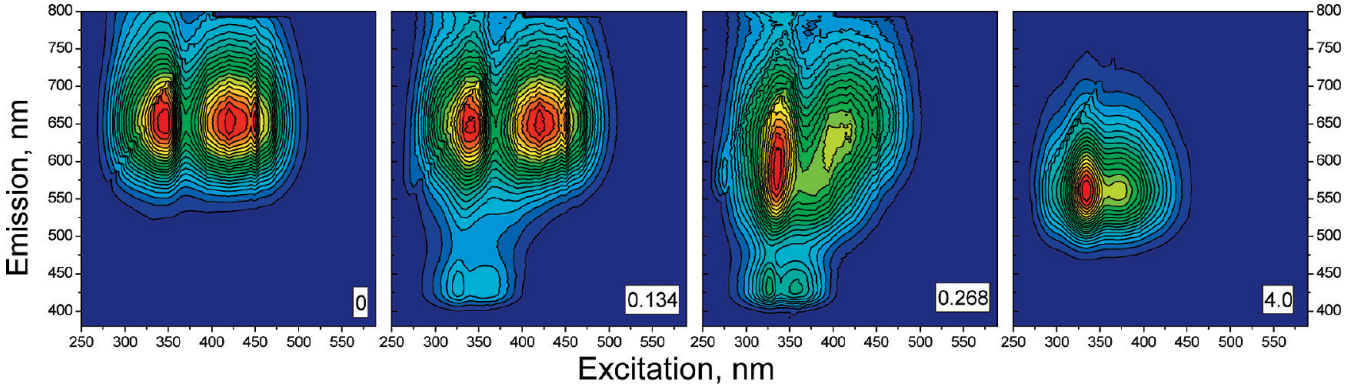

FIGURE 8. Excitation/emission contour plots of XF **4** in acetonitrile in the presence of various amounts of TFA (mM, bottom right corner of each graph). The difference between the neighboring lines corresponds to the constant intensity difference on a linear scale. Red color corresponds to higher intensities.

TABLE 1. Log β Values for the Protonation of 1−5 by TFA in Acetonitrile

		−log β	
XF	basic group	absorption	emission
1	NBu_2	4.06	4.12
2	Pyr	4.08	4.10
3	NBu_2	3.93	3.74
4	Pyr/NBu_2	5.1/3.41	5.08/3.30
5	Pyr	4.41	4.38

work we have exposed **1**−**5** to different metal triflates in either dichloromethane or acetonitrile and investigated the metal-induced changes of absorption and fluorescence in **1**−**5** (Table 2).

Interaction of the XFs with Metal Ions. Main-group metal ions and metal cations with d^0, d^5, and d^{10} configurations act typically as positive point charges and in that (and only that) respect are similar to protons. Our experience with XFs **6**−**8** shows that some ligands are capable of coordinating metal ions with concomitant change of emission color. We were interested in evaluating if the unsymmetrical XFs **1**−**5** would respond similarly to metal ions as their symmetric congeners **6**−**8**. Figure 9 displays a photograph of solutions of **1**−**5** in dichloromethane before and after addition of 10 different metal triflates at saturation. The pictures were taken under black light illumination at λ = 366 nm. While the addition of lithium and potassium triflate salts does not lead to any fluorescence change, the other cations elicit differential changes in **1**−**5**. The changes are qualitatively similar to those observed for protonation but do not occur for each XF with each metal.

Figure 10 displays the corresponding selected absorption and emission spectra. In the case of XF **1**, Mg^{2+}, Ba^{2+}, Mn^{2+}, Ag^{+}, Zn^{2+}, and Sn^{2+} all lead to a blue shift in emission, as expected for a coordination of the aniline nitrogens. Cu^{2+} leads to a pink or purple emission, which results from dual emission from the complexed and the

TABLE 2. Optical Properties of the XFs 1−5

	1			2			3			4			5		
metal ion	absorption λ_{max} (nm)	emission λ_{max} (nm)	Φ	absorption λ_{max} (nm)	emission λ_{max} (nm)	Φ	absorption λ_{max} (nm)	emission λ_{max} (nm)	Φ	absorption λ_{max} (nm)	emission λ_{max} (nm)	Φ	absorption λ_{max} (nm)	emission λ_{max} (nm)	Φ
none	314, 423	538	0.183	328	447	0.521	315, 447	585	0.079	312, 441	578	0.075	313, 423	548	0.294
Li^+	318, 422	540 (433, 451)	0.283	327	449	0.407	315, 447	583	0.085	317, 450	578 (431)	0.044	313, 423	547	0.277
K^+	316, 423	538	0.183	328	447	0.512	316, 448	585	0.082	310, 442	578	0.072	313, 422	548	0.285
Mg^{2+}	328	433	0.738	307, 331, 412	558	0.097	315, 447	583	0.082	328	527	0.156	313, 423	549	0.286
Ca^{2+}	320, 421	539 (433, 451)	0.311	327	447	0.441	315, 449	581 (441)	0.090	311, 446	577 (432)	0.056	314, 426	547	0.226
Ba^{2+}	329	435	0.666	307, 332, 411	559	0.098	331	435	0.757	328	527	0.153	326, 486	NF	
Mn^{2+}	328	434	0.662	307, 332, 408	558	0.099	330	435	0.700	329	526	0.127	327, 489	NF	
Cu^{2+}	329	433	0.560	306, 332, 410	558	0.124	320	435 (587)	0.428	326	525	0.085	312 (480)	NF	
Ag^+	328	434	0.580	307, 332, 406	558	0.089	331	450	0.612	326, 402	518	0.050	326, 488	NF	
Zn^{2+}	328	433	0.726	308, 331, 406	557 (433)	0.107	330	435	0.554	327	525	0.155	327, 485	NF	
Sn^{2+}	329	433	0.656	307, 332, 410	558	0.098	331	435	0.758	327	526	0.133	326, 489	NF	
H^+	326	436	0.767	306, 334, 410	560	0.097	331	438	0.758	333, 381	527	0.196	326, 486	NF	

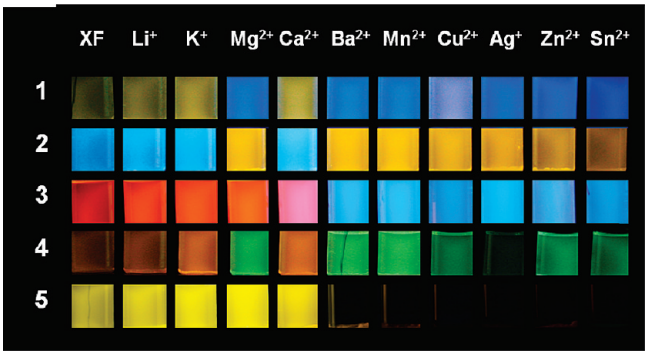

FIGURE 9. Panel of the exposure of XFs **1**−**5** toward an excess of different metal triflates in dichloromethane. The photograph was taken using a hand-held UV−vis lamp with a λ_{max} of 366 nm against a black background.

uncomplexed forms. In **2**, coordination of the pyridine group results in a lowering of the LUMO and a yellow-orange emission for all cations with exception of Li^+, K^+, and Ca^{2+}. XF **3**, while its absorption and emission are red-shifted, displays qualitatively the same emission characteristics as **1** upon treatment with metal cations but a red to blue shift is observed. Metals that coordinate to **4**, induce a shift from red to green, while in the case of **5**, which should be analogous to **2**, yellow emission is apparent; however, once the metal ions or protons coordinate(s), the emission of **5** is fully quenched.

According to Figure 10, changes in absorption and emission upon coordination of an XF to metal cations are in most cases similar to changes observed upon protonation, even though in the case of metal cations some do not bind at all, such as Li^+ or Ca^{2+} to XF **1** in dichloromethane, and some XF−metal−salt combinations lead to an equilibrium of bound and unbound XF. In acetonitrile, the concentration of calcium triflate at least can be pushed sufficiently high to allow close to full coordination of the XF to the Ca^{2+} ions. To further investigate these phenomena and obtain a more quantitative picture, we titrated **4** with both manganese triflate and with calcium triflate in acetonitrile (Figures 11 and 12). In principle, these data look very similar to those obtained for the titration of **4** with trifluoroacetic acid; however, attempts to fit the data by SVD were unsuccessful, suggesting that additional equilibria must exist which are difficult to simulate and play a significant role in these two cases. Qualitatively though, one observes the same features as in the protonation study. A red shift in absorption, as a testament to the coordination to the pyridine arm of the XF **4**, is mirrored by a blue shift in emission and is apparently counterintuitive but easy to understand if one looks at the equilibria displayed in Figure 7. In the event that the metal cation is bound to the pyridine, the resulting species is nonfluorescent and red absorptive, while if the aniline moiety is metal coordinated a species forms that will not display any easily detected changes in absorption but will emit in the blue. Excited-state decomplexation, or enhanced photoacidity, however, does not seem to be prevalent in any of the studied XFs, as the lockstep of the changes in absorption and emission delineates.

However, to obtain binding constants of the XFs to metal cations we performed a titration of XF **1** in acetonitrile with both manganese and calcium triflates. As in this case only one binding site is available, complications that would result from the presence of multiple binding sites are excluded. Figures 13 and 14 and Table 3 display the details. The XF **1** is well-behaved, and we were able to extract binding constants from both the absorption and the emission spectra by deconvolution of the titration traces by the singular value decomposition (SVD). According to these data, $\log \beta_{Mn} = 3.8$ from absorption data and $\log \beta_{Mn} = 4.0$ from the emission data. A similar trend but much smaller numerical values are obtained for calcium triflate $\log \beta_{Ca} = 1.8$ from absorption data and $\log \beta_{Ca} = 1.6$ from the emission data. In both cases, the binding constants derived from absorption and emission are remarkably close, so that one can conclude that excited-state decomplexation does not play a significant role for distyrylbenzenes, at least not under the conditions employed herein.

Conclusion

We have synthesized the hitherto unknown XFs **1**−**5** by a sequential double-Horner reaction followed by a Sonogashira coupling and compared their properties to those of the symmetrical XFs **6**−**8**. We have investigated the issue of the photoacidity of these XFs as well as of that of the metallochromicity of the XFs, and we find that they neither display excited-state decomplexation nor enhanced photoacidity. This is somewhat contrary to the general belief and to chemical intuition that stilbene types should show enhanced photoacidity and excited-state decomplexation due to the significant participation of quinoidal resonance

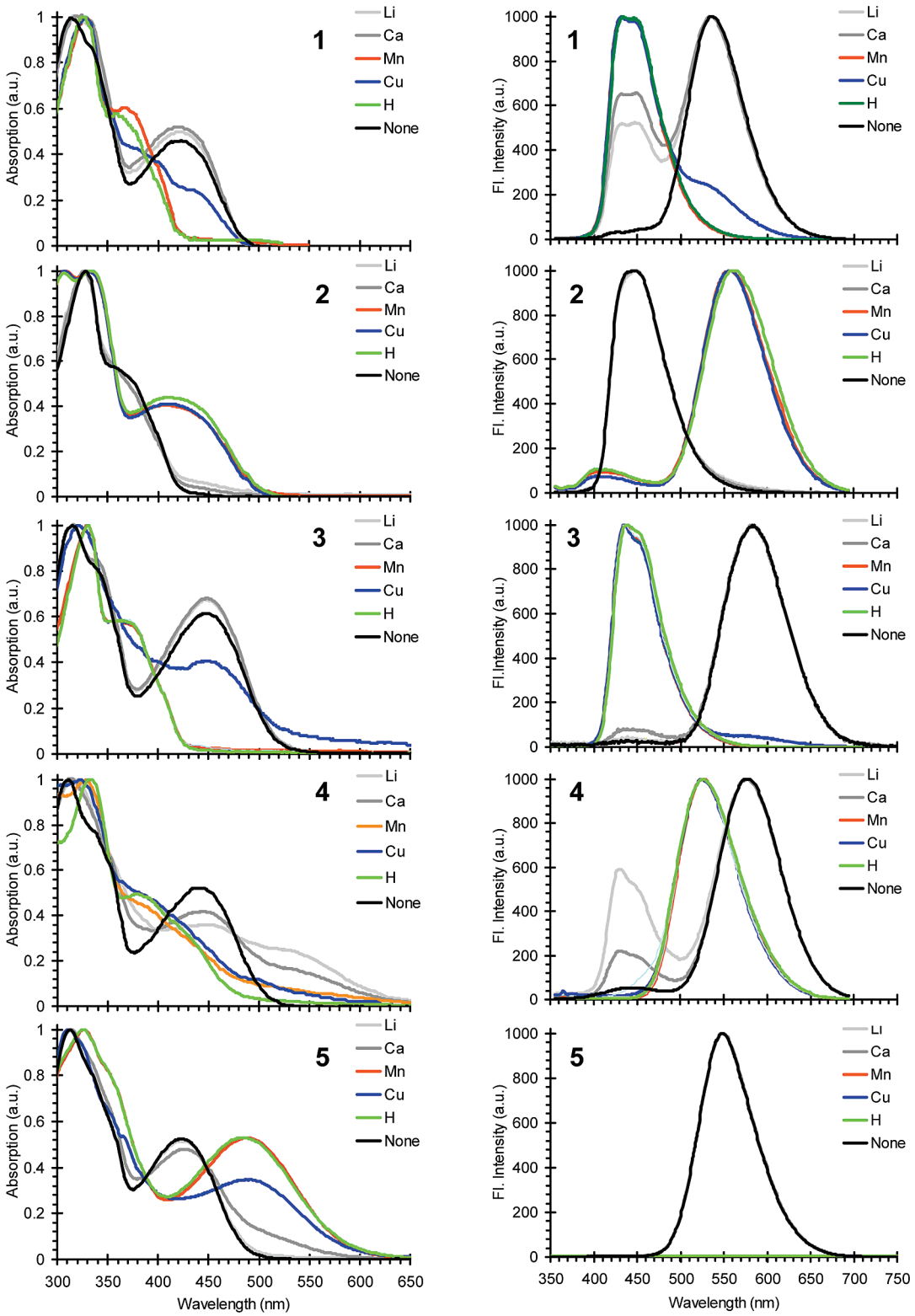

FIGURE 10. UV/vis absorption and emission spectra of **1**−**5** in the presence of protons and selected metal triflates in dichloromethane as solvent. On the left-hand side absorption data are shown, while on the right-hand side the emission data are displayed. The excitation wavelength was 350 nm.

structures in the excited state. Our results are, however, in full agreement with our earlier results that distyrylbenzenes and their derivatives have a significantly different photophysics and photochemistry from stilbenes.[22,23] We also notice that in donor−acceptor substituted distyrylbenzenes, and XFs

(22) Solntsev, K. M.; McGrier, P. L.; Fahrni, C. J.; Tolbert, L. M.; Bunz, U. H. F. *Org. Lett.* **2008**, *10*, 2429–2432.

(23) (a) Lewis, F. D.; Sinks, L. E.; Weigel, W.; Sajimon, M. C.; Crompton, E. M. *J. Phys. Chem. A* **2005**, *109*, 2443–2451. (b) Crompton, E. M.; Lewis, F. D. *Photochem. Photobiol. Sci.* **2004**, *3*, 660–668. (c) Lewis, F. D.; Crompton, E. M. *J. Am. Chem. Soc.* **2003**, *125*, 4044–4045.

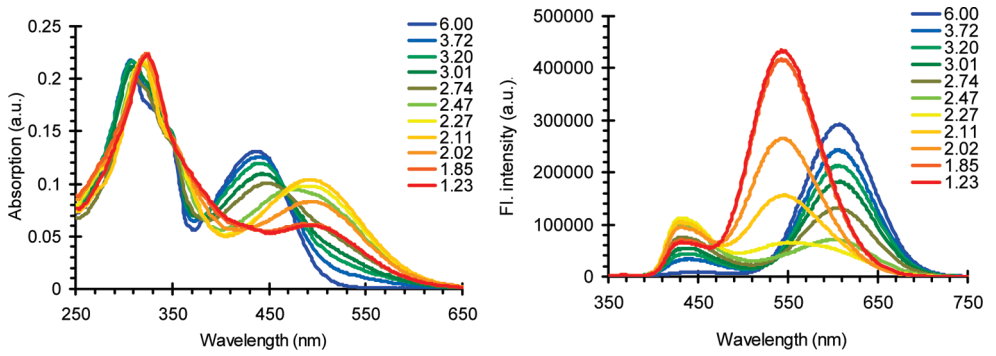

FIGURE 11. Titration of XF **4** in acetonitrile with calcium triflate: (left) UV/vis absorption; (right) emission. The inset displays the concentration $-\log[Ca^{2+}]$ in mol L^{-1}. Notice that in acetonitrile the final concentration of calcium triflate can be pushed considerably higher. As a consequence, close to full metalation of the XF **4** is possible and there is no uncomplexed XF left. The excitation wavelength was 350 nm.

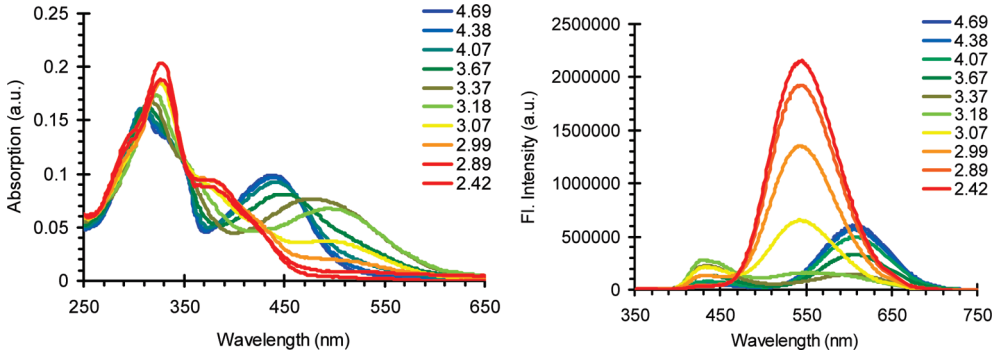

FIGURE 12. Titration of XF **4** in acetonitrile with manganese triflate: (left) UV/vis absorption; (right) emission. The inset displays the concentration $-\log[Mn^{2+}]$ in mol L^{-1}. The excitation wavelength was 350 nm.

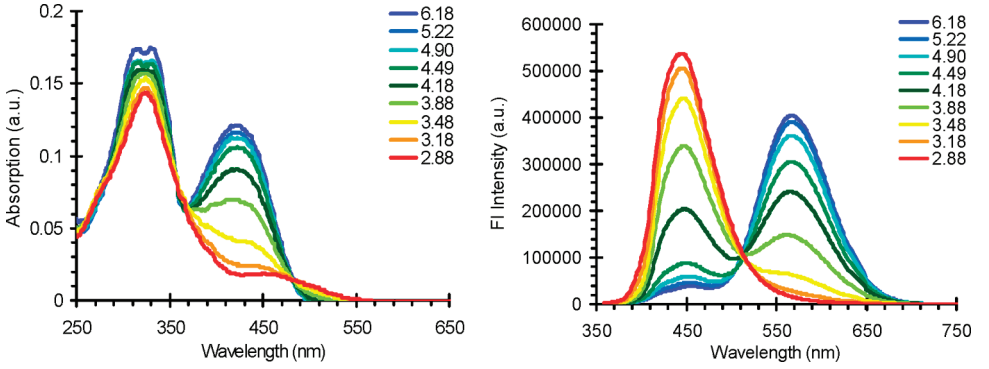

FIGURE 13. Titration of XF **1** in acetonitrile with manganese triflate: (left) UV/vis absorption; (right) emission. The inset displays the concentration $-\log[Mn^{2+}]$ in mol L^{-1}. The excitation wavelength was 350 nm.

TABLE 3. Binding of the XFs 1 to Calcium and Manganese Triflates

	-Log β	
	absorption	amission
Mn^{2+}	3.79	3.98
Ca^{2+}	1.75	1.56

are a special case of distyrylbenzenes, the substitution pattern, i.e., where the acceptor is located, seems to be critical. Indeed, Perry, Marder et al. demonstrated that 2,5-dicyano-1,4-distyrylbenzenes show little cation-induced shift in emission upon metal coordination.[10a] All the cases we have investigated, however, show quite large shifts in absorption and emission. Exceptions are water-soluble EDTA-like XFs, in which aqueous solutions of metal salts disrupt excimers of these fluorophores but do not lead to significant shifts in absorption.[24] We suspect that the presence of the electron-accepting $-CH_2CO_2^-$ groups has a detrimental influence on the basicity of the aniline nitrogen, and coordination of metal cations will not occur through them. In the case of **1**−**4**, even in polar solvents such as acetonitrile, coordination to metal cations leads to significant changes in absorption and particularly in emission; addition of suitable electronically nondisturbing binding appendages to the amine groups of the XFs should lead then perhaps to functional metal

(24) Tolosa, J.; Zucchero, A. J.; Bunz, U. H. F. *J. Am. Chem. Soc.* **2008**, *130*, 6498–6506.

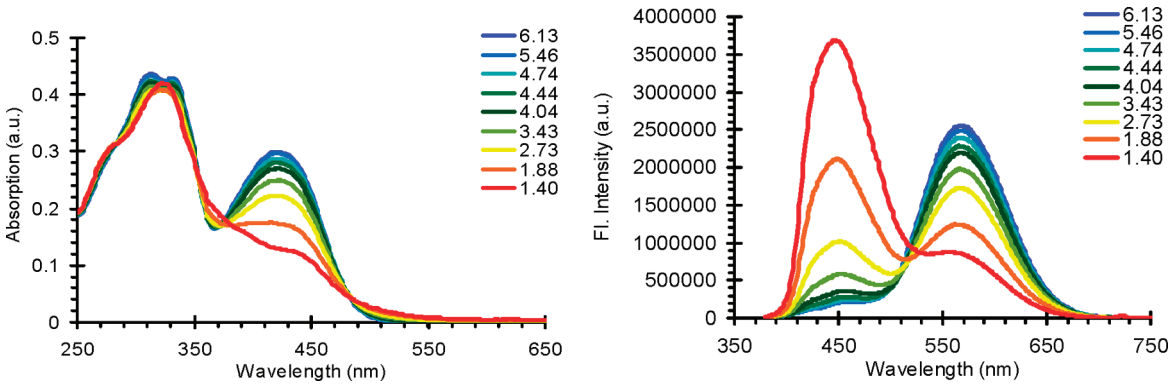

FIGURE 14. Titration of XF **1** in acetonitrile with calcium triflate: (left) UV/vis absorption; (right) emission. The inset displays the concentration $-\log[Ca^{2+}]$ in mol L^{-1}. The end of the titration is defined by the saturation of the solution with calcium triflate. Full coordination of **1** to calcium triflate is not possible. The excitation wavelength was 350 nm.

sensory XFs that can be deployed in cell staining and other biosensory applications.

Experimental Section

(*E*)-1-[4-Di(1-butyl)aminostyryl]-(*E*′)-4-(4-*tert*-butylstyryl)-2,5-bis(phenylethynyl)benzene 1 (General Procedure C). A solution of **13** (141 mg, 0.252 mmol), $PdCl_2(PPh_3)_2$ (2%) and CuI (2%) in 3 mL of a mixture of dry THF/piperidine 2:1 was stirred for 10 min at room temperature under N_2. Phenylacetylene (257 mg, 2.52 mmol) was added and the reaction was stirred at room temperature overnight. After reaction time, the mixture was poured into water and extracted with dichloromethane (DCM) (3 × 25 mL). The combined organic phases were collected and dried over $MgSO_4$, and the solvent was evaporated after filtration. The crude mixture was purified by column chromatography (hexanes/ethyl acetate 9:1) to provide an orange solid (145 mg, 87%). Mp: 78−81 °C. ^{1}H NMR, $CDCl_3$ (δ, 300 MHz): 0.97 (t, 6H, J = 7.2 Hz); 1.33−1.42 (m, 4H); 1.35 (s, 9H); 1.54−1.66 (m, 4H); 3.31 (t, 4H, J = 7.5 Hz); 6.65 (d, 2H, J = 9 Hz,); 7.20 (d, 1H, J = 16 Hz,); 7.24 (d, 1H, J = 16 Hz); 7.38−7.48 (m, 11H); 7.52 (d, 2H, J = 9 Hz); 7.60−7.68 (m, 5H); 7.89 (broad s, 2H). ^{13}C NMR, $CDCl_3$ (δ, 75 MHz): 151.3, 148.3, 138.6, 136.7, 134.9, 131.8, 131.2, 130.0, 128.9, 128.8, 128.7, 128.6, 128.5, 128.4, 128.4, 126.7, 126.7, 125.9, 125.3, 124.6, 123.6, 123.5, 122.3, 121.7, 120.5, 111.8, 95.3, 95.3, 88.5, 88.3, 51.0, 34.9, 31.5, 29.7, 20.6, 14.3. IR (cm^{-1}): 3037, 2956, 2863, 1604, 1577, 1517, 1511, 1364, 1181, 958.6, 807, 754, 690. MS (EI): (M^+) 665. HRMS: 665.3983 (calcd 665.3974). Anal. C, 89.90; H, 8.02; N, 2.15 (calcd C, 90.18; H, 7.72; N, 2.10).

(*E*)-1-[2-(Pyridin-4-yl)vinyl]-(*E*′)-4-[4-di(1-butyl)aminostyryl]-2,5-bis(phenylethynyl)benzene 4. We employed general procedure C, using diiodide **16** (331 mg, 0.499 mmol). The crude mixture was purified by precipitation in cold ethanol to give an orange solid (256 mg, 84%). Mp: 138−142 °C. ^{1}H NMR, CD_2Cl_2 (δ, 300 MHz): 0.97 (t, 6H, J = 7.2 Hz); 1.33−1.42 (m, 4H); 1.54−1.67 (m, 4H); 3.32 (t, 4H, J = 7.5 Hz); 6.66 (d, 2H, J = 9 Hz,); 7.20 (d, 1H, J = 16 Hz,); 7.25 (d, 1H, J = 16 Hz); 7.40−7.50 (m, 2H); 7.60−7.69 (m, 6H); 7.88 (d, 1H, J = 16 Hz,); 7.93 (broad s, 2H). ^{13}C NMR, CD_2Cl_2 (δ, 75 MHz): 150.6, 148.8, 144.8, 139.9, 135.1, 132.3, 131.9, 130.2, 129.7, 129.1, 129.0, 128.9, 128.9, 128.6, 128.4, 127.6, 124.1, 123.5, 123.2, 123.1, 121.8, 121.2, 119.7, 111.9, 96.0, 95.8, 88.1, 87.8, 51.0, 29.8, 20.7, 14.1. IR (cm^{-1}): 2968, 2868, 1593, 1582, 1522, 1497, 1365, 1181, 961, 803, 756, 686. MS (EI): (M^+) 610, HRMS: 610.3302 (calcd 610.3314). Anal. C, 88.52; H, 6.87; N, 4.64 (calcd C, 88.48; H, 6.93; N, 4.59).

(*E*)-Diethyl 2,5-Diiodo-4-[4-di(1-butyl)aminostyryl]benzylphosphonate 10 (General Procedure for Horner Monoalkenylation A). A solution of diphosphonate **9**[25] (3.15 g, 5.00 mmol) in dry THF (75 mL) was stirred at 0 °C under N_2 while ^{t}BuOK (505 mg, 4.50 mmol) was added carefully. After addition, the reaction mixture was stirred for 3 min. Then, 4-di(1-butyl)aminobenzaldehyde (933 mg, 4.00 mmol) in dry THF (5 mL) was added as quickly as possible. After 30−40 min, 75 mL of water, followed by 5 mL of an aqueous saturated solution of NH_4Cl, was added to quench the reaction. The mixture was extracted with DCM (3 × 75 mL). The combined organic phases were washed with water and brine and dried over $MgSO_4$. After filtration, the solvent was removed in vacuo and the crude mixture was purified by column chromatography (ethyl acetate/hexanes 1:2) to give **10** as a yellow oil (1.39 g, 49%). ^{1}H NMR, $CDCl_3$ (δ, 300 MHz): 0.97 (t, 6H, J = 7.2 Hz); 1.28 (t, 6H, J = 7.2 Hz); 1.30−1.40 (m, 4H); 1.49−1.60 (m, 4H); 3.20−3.32 (m, 6H); 3.97−4.14 (m, 4H); 6.57 (d, 2H, J = 9 Hz); 6.83 (d, 1H, J = 16 Hz); 6.89 (d, 1H, J = 16 Hz); 7.39 (d, 2H, J = 9 Hz); 7.79 (d, 1H, J = 4 Hz); 7.98 (d, 1H, J = 2 Hz). ^{13}C NMR, $CDCl_3$ (δ, 75 MHz): 148.5, 141.8 (d, J = 3.2 Hz), 140.7 (d, J = 6.4 Hz), 135.8 (d, J = 3.1 Hz), 135.0 (d, J = 9.6 Hz), 133.0, 128.6, 125.0, 123.5, 111.7, 101.6 (d, J = 7.2 Hz), 99.7 (d, J = 4.0 Hz), 62.7 (d, J = 7.2 Hz), 51.0, 37.6 (d, J = 137 Hz), 29.6, 20.5, 16.8 (d, J = 5.6 Hz), 14.3. The synthesis of **9** provides a partially brominated impurity which is impossible to separate from the desired compound.[25] This makes impossible to obtain elemental analysis for the precursors of XFs **1**−**5**.

(*E*)-1-[4-Di(1-butyl)aminostyryl]-(*E*′)-4-(4-*tert*-butylstyryl)-2,5-diiodobenzene 13 (General Procedure B). A solution of **12** (1.29 g, 2.03 mmol) and 4-di(1-butyl)aminobenzaldehyde (520 mg, 2.23 mmol) in dry THF (25 mL) was stirred at 0 °C under N_2 while ^{t}BuOK (250 mg, 2.23 mmol) was added carefully. After addition, the reaction mixture was stirred for 30 min. Then, 20 mL of water followed by 3 mL of a saturated aqueous solution of NH_4Cl was added to quench the reaction. The mixture was extracted with DCM (3 × 50 mL). The combined organic phases were washed with water and brine and dried over $MgSO_4$. The crude mixture was purified by column chromatography (ethyl acetate/hexanes 1:9) to give **13** as a yellow solid (1.20 g, 83%). Mp: 135−139 °C. ^{1}H NMR, $CDCl_3$ (δ, 300 MHz): 0.97 (t, 6H, J = 7.2 Hz); 1.33−1.42 (m, 4H); 1.35 (s, 9H); 1.54−1.66 (m, 4H); 3.31 (t, 4H, J = 7.5 Hz); 6.65 (d, 2H, J = 9 Hz,); 6.85−7.00 (m, 2H); 7.16 (d, 1H, J = 16 Hz,); 7.35−7−55 (m, 7H); 8.01 (broad s, 2H). ^{13}C NMR, $CDCl_3$ (δ, 75 MHz): 151.4, 148.4, 141.5, 139.7, 136.1, 135.5, 134.0, 132.6, 131.4, 129.9, 128.5, 126.7, 125.2, 123.6, 111.5, 100.4, 100.1, 51.0, 34.9, 31.5, 29.8, 20.7, 14.1. IR (cm^{-1}): 3030, 1605, 1518, 1364, 961, 735. MS (EI): (M^+) 717.

(25) Wilson, J. N.; Windscheif, P. M.; Evans, U.; Myrick, M. L.; Bunz, U. H. F. *Macromolecules* **2002**, *35*, 8681–8683.

Acknowledgment. We thank the National Science Foundation for generous support (U.B., J.T. NSF CHE 0750275 Cruciform Fluorophores; LMT and KMS NSF CHE-0809179 excited-state proton transfer). J.T. thanks the Junta de Comunidades de Castilla La Mancha (Fondo Social Europeo FSE 2007-2013) for his postdoctoral grant. We thank Profs J.-S. Yang and W. Rettig for valuable comments. We thank Katya Kouznetsova for the covert art design.

Supporting Information Available: Spectroscopic data and synthetic details. This material is available free of charge via the Internet at http://pubs.acs.org.